An integrated modelling approach for assessing the effect of multiscale complexity on groundwater source yields

Upton, K.A.[a]*, Jackson, C.R.[b], Butler, A.P.[c], Jones, M.A.[d]

[a]British Geological Survey, The Lyell Centre, Research Avenue South, Edinburgh EH14 4AP, UK

[b]British Geological Survey, Environmental Science Centre, Keyworth, Nottingham, NG12 5GG, UK

[c]Department of Civil and Environmental Engineering, Imperial College London, SW7 2AZ, UK

[d]Thames Water Utilities Ltd, Clearwater Court, Vastern Road, Reading, RG1 8DB, UK

*Corresponding author: kirlto@bgs.ac.uk +44 (0)131 650 0210

ABSTRACT

A new multi-scale groundwater modelling methodology is presented to simulate pumped water levels in abstraction boreholes within regional groundwater models, providing a robust tool for assessing the sustainable yield of supply boreholes and improving our understanding of groundwater availability during drought. A 3D borehole-scale model, which solves the Darcy-Forchheimer equation in cylindrical co-ordinates to simulate both linear and non-linear radial flow to a borehole in a heterogeneous aquifer, is embedded within a Cartesian grid, using a hybrid radial-Cartesian finite difference method. The local-scale model is coupled to a regional groundwater model, ZOOMQ3D, using the OpenMI model linkage software, providing a flexible and efficient tool for assessing the behaviour of a groundwater source within its regional hydrogeological context during historic droughts and under climate change. The advantages of the new method are demonstrated through application to a Chalk supply borehole in the UK.

KEYWORDS

Water resources, groundwater, sustainable yield, multiscale modelling, OpenMI

SOFTWARE AVAILABILITY

Name of software: SPIDERR; Developer: Dr Kirsty Upton (kirlto@bgs.ac.uk); Availability: On request; Program language: MATLAB

DECLARATION OF INTEREST

We wish to confirm that there are no known conflicts of interest associated with this publication and there has been no significant financial support for this work that could have influenced its outcome.

1. INTRODUCTION

Groundwater plays a significant role in providing water for domestic, agricultural and industrial use worldwide (WWAP, 2015), but around 20% of the world's aquifers are estimated to be over-exploited (Gleeson et al., 2012). As pressures on global water resources increase due to climate change and population growth, the sustainable management of groundwater resources becomes more critical. Preventing over-exploitation and subsequent reductions in long-term groundwater availability at the aquifer scale requires an understanding of the relationship of demand for groundwater abstraction with the environmental role of groundwater in delivering ecosystem services within the context of long-term average recharge. Over shorter time-scales, effective water resource management also requires an understanding of the sustainable yield of individual abstraction boreholes during drought. This is particularly important in aquifers where there are seasonal groundwater level fluctuations and where groundwater abstractions impact on other wells and the surrounding environment. Water resource managers therefore require

tools to allow evaluation of short- and long-term groundwater availability, at both the aquifer scale and at the scale of individual boreholes, and how external stresses such as climate change and increasing demand might impact the availability of groundwater at these different spatial and temporal scales.

Numerical groundwater models provide invaluable tools to investigate the response of aquifers to different environmental stresses (Singh, 2014). There are several examples in the literature of numerical models used for simulating the groundwater level response in a borehole. The Multi-Node Well package (Konikow et al., 2009) enables the representation of boreholes that are open to multiple aquifers in MODFLOW (McDonald & Harbaugh, 1988). This scheme uses the steady-state equation of flow towards a borehole (Thiem, 1906) to correct for the difference in head between that simulated on a low resolution Cartesian grid and that in a borehole. The main advantage of this approach is that it is a computationally efficient way of including abstractions in regional groundwater models because it does not refine the model mesh around the borehole. However, is it often found that heterogeneity and hydrogeological complexity close to boreholes control their behaviour (Rushton & Rathod, 1988; Tamayo-Mas et al., 2018; Upton et al., 2019). Consequently, most studies that have aimed to simulate fluctuations in within-borehole water levels and their performance accurately have applied numerical ‘radial flow’ models (Rushton & Booth, 1976; Connorton & Reed, 1978; Rushton & Weller, 1985; Rathod & Rushton, 1991; Rushton, 2006; Konikow et al., 2009; Mathias & Todman, 2010; Mansour et al., 2011; Upton et al., 2019). These models are typically based on a radial grid structure to simulate flow converging to an abstraction borehole. They represent the small-scale features and groundwater flow processes that are required to reproduce the groundwater level response within an individual borehole (typically at spatial scales of less than 1m), including the effects of borehole storage, well casing and screening, vertical aquifer heterogeneity, seepage face

development, and non-Darcian flow. Radial flow models do not generally provide an adequate representation of regional groundwater flow processes. In contrast, there are numerous examples in the literature of distributed groundwater models, which represent large-scale features and processes such as regional recharge patterns and geological heterogeneity, that have been applied to regional water resource assessment and management problems in various geographical, climatic, and hydrogeological settings (Rushton et al., 1989; Salmon et al., 1996; Ebraheem et al., 2004; Al-Salamah et al., 2011; Jackson et al., 2011; Shepley et al., 2012; Sherif et al., 2012; Eissa et al., 2013; Mohamed et al., 2016). Regional models typically assign abstraction boreholes to single grid cells, which may be on the scale of several tens, hundreds, or even thousands of meters, leading to large discretization errors in the vicinity of the borehole. There are few examples in the literature of multi-scale numerical groundwater models that allow a detailed representation of individual abstraction boreholes within regional-scale groundwater models (Abrams et al., 2016; Feinstein et al., 2016).

Numerical groundwater models typically use finite difference (FDM), finite volume (FVM), or finite element methods (FEM) to solve the governing partial differential equation (Wang & Anderson, 1982). These methods take different approaches to simulating flow across multiple scales. In widely applied FDM groundwater modelling codes such as ZOOMQ3D (Jackson & Spink, 2004) and earlier versions of MODFLOW (McDonald & Harbaugh, 1988), local grid refinement (LGR) methods (von Rosenberg, 1982; Szekely, 1998; Jackson, 2000; Mehl & Hill, 2002; Mehl & Hill, 2004) allow a more accurate solution in regions with rapidly changing hydraulic gradients, such as in the vicinity of abstraction boreholes, but are limited to square or rectangular grids. Outside the field of groundwater modelling, a hybrid radial-Cartesian FDM has been applied to simulate production wells in petroleum reservoir models (Akbar, 1974; Mrosovsky, 1974; Pedrosa Jr & Aziz, 1986; Gottardi, 1990). In this method, one or more grid

cells of the regional model is replaced by a radial grid allowing grid refinement down to the diameter of the well. The conductance term of the irregular shaped blocks at the boundary between the radial and Cartesian grids is determined by substituting the irregular block with a fictitious radial or rectangular block with the same volume and hydraulic properties. This conserves mass but assumes that potential is uniform across the irregular volume, flow is orthogonal across the outer boundary of the irregular block, and the principal directions of permeability are aligned with the co-ordinate axes thus not dealing with full tensor anisotropy.

The FVM and FEM, which are based on unstructured grids, allow a smooth transition between coarse and fine grid scales without complex boundary conditions at a grid interface, as is the case in the LGR and hybrid radial-Cartesian methods. These methods provide greater geometric flexibility but grids can be more time-consuming to construct and may result in models that are computationally more demanding to solve. The FVM based on a two-point flux approximation, often referred to as the control volume finite difference (CVFD) method, has recently been applied in MODFLOW-USG (Panday et al., 2013) and MODFLOW 6 (Hughes et al., 2017; Langevin et al., 2017). It has also been used in multi-scale petroleum reservoir (Rozon, 1989; Heinemann, 1991; Palagi, 1993; Palagi, 1994; Palagi & Aziz, 1994) and atmospheric models (Ringler et al., 2008; Ju et al., 2010; Ringler et al., 2013). The CVFD method requires grids to be locally orthogonal and, like the FDM, does not account for full-tensor anisotropy, although this is accommodated in MODFLOW 6 through the XT3D package (Provost et al., 2017). The multi-point flux approximation FVM and FEM can incorporate full-tensor anisotropy, and are applied on fully unstructured grids providing the highest level of geometric flexibility. The FVM methods have been applied to multi-scale problems in petroleum reservoir, atmospheric and oceanic modelling (Aavatsmark et al., 1996; Ding & Jeannin, 2001;

123 Aavatsmark, 2002; Chen et al., 2003; Mundal et al., 2010; Neale et al., 2010), while the FEM is
124 used in the FEFLOW groundwater modelling code (Diersch, 2002).
125
126 Hiebert *et al.* (1993) and Fung *et al.* (1994) compare the discretization schemes described
127 above (refined Cartesian, hybrid radial-Cartesian, refined CVFD, as well as a hybrid radial-
128 CVFD scheme) for simulating near-well processes in regional petroleum reservoir models. They
129 show that a radial scheme provides the greatest accuracy and efficiency for simulating near-well
130 processes, compared with the refined Cartesian or CVFD schemes and that, while the hybrid
131 radial-CVFD grid provides greater flexibility and accuracy across the boundary than the hybrid
132 radial-Cartesian grid, the results from these two schemes are comparable. Comparison of the
133 two-point and multi-point flux approximation FVMs show that the multi-point scheme is less
134 computationally efficient and only necessary for highly anisotropic simulations (Mundal et al.,
135 2010).
136
137 The review above does not contain an exhaustive summary of all potential methods for
138 modelling groundwater from the regional to the local (borehole) scale, but covers the most
139 commonly applied numerical approaches. Alternative approaches, such as the analytical
140 element, mesh-free, and lattice Boltzmann methods have gained increased attention in the
141 literature but have had limited uptake within the groundwater community (Li et al., 2002; Anwar
142 et al., 2008; Anwar & Sukop, 2009b; Anwar & Sukop, 2009a; Bandilla et al., 2009; Wen et al.,
143 2014).
144
145 When considering the specific example of representing individual boreholes within a regional
146 groundwater model, the task of constructing, solving, and calibrating a large-scale model
147 containing refined sub-regions around multiple abstraction boreholes would be both challenging

and time-consuming. An alternative approach is to link or couple two different models, specifically developed for simulating groundwater flow processes at different scales: a regional model for representing catchment-scale processes and a small-scale model for simulating flow processes local to a borehole. Model linkage standards, such as OpenMI (Moore & Tindall, 2005; Gregersen et al., 2007) and the Community Surface Dynamics Modeling System (Peckham et al., 2013), provide such methods for linking models at different scales in a relatively straightforward way. OpenMI was developed in response to the EU Water Framework Directive, which requires an integrated, catchment-scale approach to water resource management. The OpenMI standard was therefore designed to enable different types of catchment models, representing processes at different spatial and temporal scales, to run simultaneously, exchanging data at run-time. It has been widely applied for linking different types of environmental models that are designed, constructed and calibrated to simulate processes at different scales (Betrie et al., 2011; Elag et al., 2011; Janssen et al., 2011; Safiolea et al., 2011; Liao et al., 2012; Butts et al., 2013; Castronova & Goodall, 2013; Castronova et al., 2013; Goodall et al., 2013; Shrestha et al., 2013; Zhou et al., 2013; Shrestha et al., 2014; Zhu et al., 2016).

This paper presents a novel methodology for linking a radial flow model with a regional groundwater model for simulating the groundwater level response in an abstraction borehole within its regional context. The multi-scale model provides a tool for water resource managers to investigate the behavior of individual abstraction boreholes within their regional context, and to run predictive scenarios to evaluate the potential impact of climate change and increasing demand on the sustainable yield of the borehole and its surrounding environment. The existing finite difference radial flow model, SPIDERR (**S**imulating **P**umping Boreholes with a **D**arcy-Forchheimer **R**egional-**R**adial Flow Model), described in detail by Upton et al. (2019), represents

the local features and flow processes required to reproduce the response in an abstraction borehole, as described above. This radial flow model is linked to the finite difference ZOOMQ3D regional groundwater modelling code through OpenMI. There are several advantages of this multi-scale modelling method for applications to water resource management: it makes use of existing regional groundwater models, which underpin groundwater resource assessment and represent a major investment; models of individual boreholes can initially be developed as standalone models without the need to run in a large regional simulation, making the calibration process more efficient; individual borehole models can then be quickly and easily linked to an existing regional groundwater model without significant time and effort required to re-grid and re-calibrate large regional-scale models (this is particularly important where multiple boreholes need to be assessed within a single regional model); the local- and regional-scale models can be run on different time-steps and over different time periods, allowing a finer temporal resolution in the local-scale model; and there is potential for this multi-scale groundwater model to be linked with other environmental models as part of an integrated approach to catchment management. This method still requires handling of the boundary between the radial and Cartesian models, which is achieved using the hybrid radial-Cartesian finite difference method described above.

The multi-scale modelling framework is described in Section 2.1, including the hybrid radial-Cartesian coupling method and the linkage of the local- and regional-scale models through OpenMI. Section 2.2 provides an evaluation of the methodology, which is then applied to a groundwater source in the Chalk aquifer in southern England (Section 3) to demonstrate the ability of the multi-scale model to accurately reproduce the response in an abstraction borehole within a regional-scale groundwater model. In the discussion (Section 4) we outline the key

benefits and limitations of the methodology, as well as potential opportunities for future development and application.

2. METHODS

2.1 Model Development

The multi-scale modelling framework links a Darcy-Forchheimer radial groundwater flow model, SPIDERR (Upton et al., 2019), with the ZOOMQ3D regional groundwater modelling code (Jackson & Spink, 2004) in two key stages, which are described in detail below: (1) within SPIDERR, the grid of the radial flow model is coupled to a Cartesian grid using the hybrid radial-Cartesian finite difference method; (2) the SPIDERR flow model is then linked to ZOOMQ3D using OpenMI.

2.1.1 Radial-Cartesian Coupling

The radial groundwater flow model, SPIDERR (Upton et al., 2019), is a 3D finite difference model based on the Darcy-Forchheimer equation for simulating linear and non-linear flow to boreholes in complex, heterogeneous aquifers. It has been shown to reproduce the groundwater level response in abstraction boreholes where drawdown is influenced by variations in borehole storage with depth, vertical heterogeneity and non-linear flow. SPIDERR's radial grid is coupled to a Cartesian grid using the hybrid radial-Cartesian finite difference method (Pedrosa Jr & Aziz, 1986). As shown in Figure 1, the radial grid effectively replaces one or more cells of the Cartesian mesh, where the location of the borehole, which is at the center of the square radial mesh, corresponds to a single node on the Cartesian mesh. This requires that the radial grid replaces a square number of Cartesian grid cells. On the radial grid, the spacing of nodes increases logarithmically in the radial direction providing greater resolution close to the borehole, where the water table has greatest curvature and is most dynamic. Each node on the

boundary of the radial grid is linked to a single node on the Cartesian grid. The radial grid must therefore comprise at least four slices in the cylindrical direction. The radial and Cartesian grids are equivalent in the vertical direction, i.e. they have the same number of layers, and these are laterally continuous across the model domain. The current model requires the Cartesian grid cells to be square and the angle of each radial slice to be equal, however it would be simple to update the model code to accommodate rectangular grids.

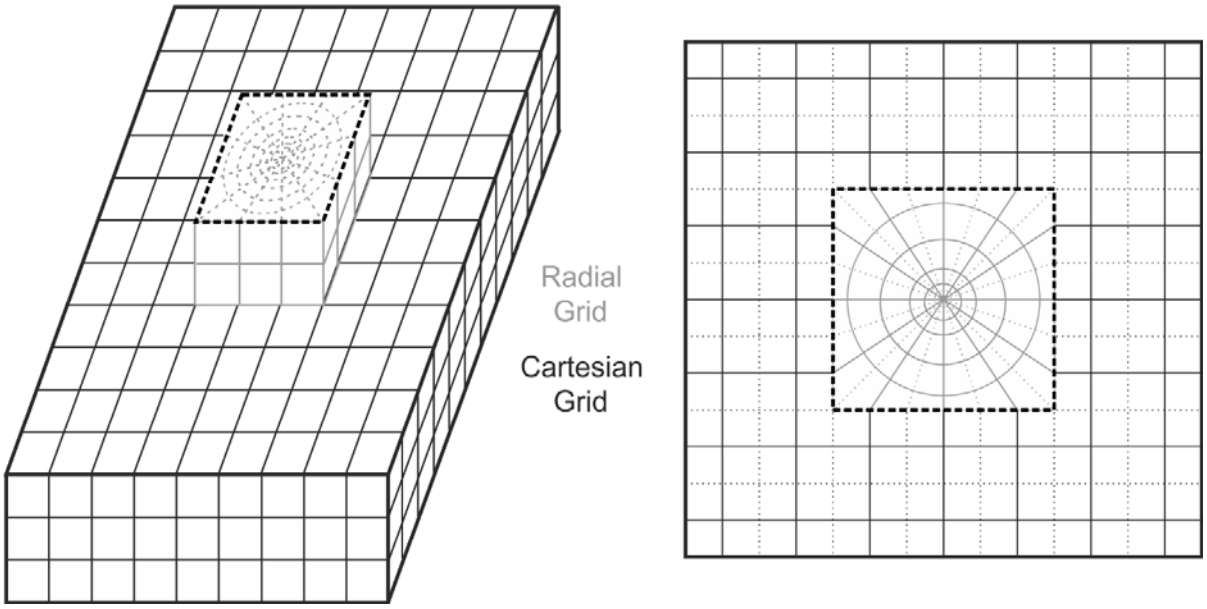

Figure 1 Conceptualization of the hybrid radial-Cartesian method used in the SPIDERR

The continuity equation for transient groundwater flow through a porous medium can be expressed in cylindrical (r, Θ, z) and Cartesian (x, y, z) coordinates as:

$$\frac{1}{r}q_r + \frac{\partial q_r}{\partial r} + \frac{1}{r}\frac{\partial q_\theta}{\partial \theta} + \frac{\partial q_z}{\partial z} = S_s\frac{\partial h}{\partial t} + N \quad (1)$$

$$\frac{\partial q_x}{\partial x} + \frac{\partial q_y}{\partial y} + \frac{\partial q_z}{\partial z} = S_s\frac{\partial h}{\partial t} + N \quad (2)$$

where q is specific discharge [LT^{-1}], S_s is specific storage [L^{-1}], t is time [T], h is hydraulic head [L], and N is a volumetric source or sink per unit volume [T^{-1}]. In SPIDERR, specific discharge (q) is calculated by the Darcy-Forchheimer equation to simulate linear and non-linear groundwater flow along each direction (l):

$$q + \beta q^2 = -K \frac{\partial h}{\partial l} \tag{3}$$

where β is the non-linear Forchheimer parameter [L^{-1}T] and K is hydraulic conductivity [LT^{-1}]. Equation 3 reduces to Darcy's Law when $\beta = 0$.

SPIDERR is based on a finite difference approximation to the continuity equation, whereby the vertical dimension is replaced by a series of layers, hydraulic head is integrated over the saturated thickness of each layer *(b)* [L], and vertical flow is calculated as a leakage term [LT^{-1}]. Specific storage is replaced by a storage coefficient (S) [-], where $S = S_s b$, except for the layer in which the water table is situated in an unconfined aquifer, where $S = S_s b + S_y$ and S_y is the specific yield [-] of the aquifer layer. Equations 1 and 2 therefore reduce to the following ordinary differential equations with respect to time, where *i, j,* and k are the node locations along the cylindrical (r, Θ, z) and Cartesian (x, y, z) directions in Equations 4 and 5, respectively:

$$S_{i,j,k} \frac{\partial h_{i,j,k}}{\partial t} = \frac{r_{i+\frac{1}{2},j,k} b_{i+\frac{1}{2},j,k} q_{i+\frac{1}{2},j,k} - r_{i-\frac{1}{2},j,k} b_{i-\frac{1}{2},j,k} q_{i-\frac{1}{2},j,k}}{r_{i,j,k}\left(r_{i+\frac{1}{2},j,k} - r_{i-\frac{1}{2},j,k}\right)} +$$

$$\frac{b_{i,j+\frac{1}{2},k} q_{i,j+\frac{1}{2},k} - b_{i,j-\frac{1}{2},k} q_{i,j-\frac{1}{2},k}}{r_{i,j,k}\Delta\theta} + q_{i,j,k+\frac{1}{2}} + q_{i,j,k-\frac{1}{2}} - N_{i,j,k} \tag{4}$$

$$S_{i,j,k}\frac{\partial h_{i,j,k}}{\partial t}=\frac{b_{i+\frac{1}{2},j,k}q_{i+\frac{1}{2},j,k}-b_{i-\frac{1}{2},j,k}q_{i-\frac{1}{2},j,k}}{\left(x_{i+\frac{1}{2},j,k}-x_{i-\frac{1}{2},j,k}\right)}+$$

$$\frac{b_{i,j+\frac{1}{2},k}\,q_{i,j+\frac{1}{2},k}-b_{i,j-\frac{1}{2},k}\,q_{i,j-\frac{1}{2},k}}{\left(y_{i,j+\frac{1}{2},k}-y_{i,j-\frac{1}{2},k}\right)}+q_{i,j,k+\frac{1}{2}}+q_{i,j,k-\frac{1}{2}}-N_{i,j,k} \quad (5)$$

Mathias *et al.* (2008) showed how Equation 3 is solved for specific discharge, which is used to calculate q in the horizontal directions in Equations 4 and 5; vertical flow is assumed to be linear and is calculated as shown by Upton et al. (2019).

Equations 4 and 5 are used to approximate groundwater head at each grid node on the radial and Cartesian meshes, respectively. The grid nodes in the irregularly shaped cells on the boundary between the two meshes (shaded grey in Figure 2), which have a curvilinear surface on the radial grid boundary and a rectilinear surface on the Cartesian grid boundary, are handled using the hybrid radial-Cartesian method outlined by Pedrosa & Aziz (1986). The hydrogeological properties and volume of the boundary cells remain constant and flows to/from the boundary nodes (i.e. nodes A, C, D and F in Figure 2) are calculated by substituting the irregular cell with a fictitious radial or Cartesian cell of equivalent volume (Figure 2). Flow between the boundary nodes and adjacent radial nodes (A and B in Figure 2a) is assumed to be radial and is calculated by substituting the irregular cell with a fictitious radial cell, whereby the new outer radius ($r^*_{i+1/2}$) is calculated from the area (a) of the irregular cell by:

$$r^{*}_{i+\frac{1}{2}}=\sqrt{\frac{2a}{\Delta\theta}+r_{i-\frac{1}{2}}{}^{2}} \quad (6)$$

The apparent radius (r^*_i) of node A is calculated as the logarithmic mid-point between $r^*_{i+1/2}$ and $r_{i-1/2}$. r^*_i *and* $r^*_{i+1/2}$ are then substituted into Equation 4 for $r_{i,j,k}$ and $r_{i+1/2,j,k}$, respectively. Flow between adjacent boundary nodes (C and D in Figure 2b) is also assumed to be radial and is calculated by substituting the irregular cells with fictitious radial cells, whereby the shifted outer radius ($r^*_{i+1/2}$) is also calculated by Equation 6 but a and $\Delta\Theta$ apply to the total area and angle of the two cells. Flow between the boundary node and adjacent Cartesian node (E and F in Figure 2c) is assumed to be orthogonal and is calculated by substituting the irregular cell with a fictitious Cartesian cell, whereby the new length (Δy^*) of the Cartesian cell, and thus position of the grid node (F), is calculated from the area *(a)* of the irregular cell by:

$$\Delta y^* = \frac{a}{\Delta x} \tag{7}$$

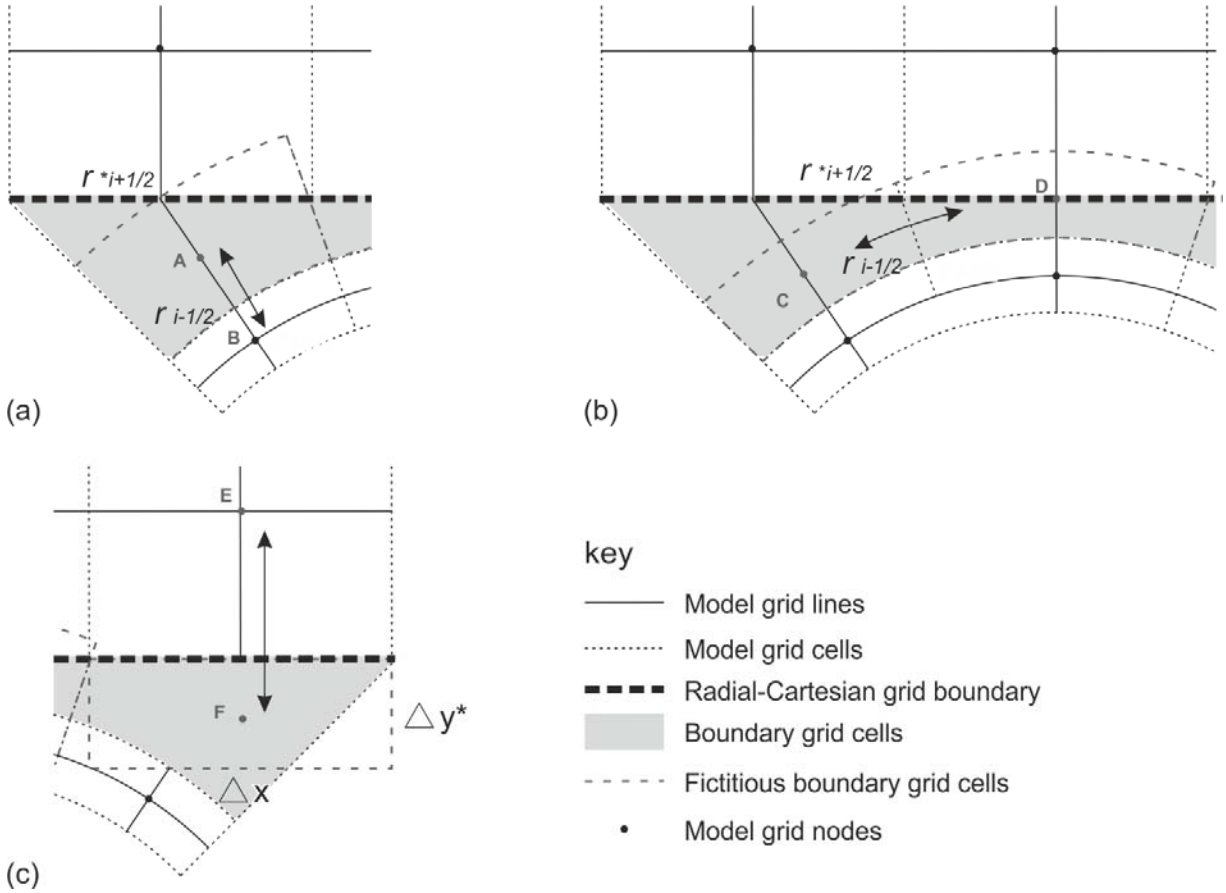

Figure 2 Conceptualisation of the radial-Cartesian boundary in SPIDERR: (a) radial flow between the boundary cell and adjacent radial cell; (b) circumferential flow between boundary cells; (c) Cartesian flow between boundary cell and adjacent Cartesian cell.

This hybrid finite difference method conserves flow across the boundary between the radial and Cartesian grids but assumes that groundwater head is uniform within the boundary cell and that flow is orthogonal across the outer boundary of the irregular cell. The errors associated with these assumptions are explored in Section 2.2. The method also allows for horizontal and vertical heterogeneity, but does not deal with full tensor anisotropy.

The SPIDERR flow model is coded using the MATLAB software package (Mathworks, 2012). The set of non-linear ordinary differential equations is solved using the stiff differential equation solver ode15s, which uses adaptive time-stepping (Shampine & Reichlet, 1997).

2.1.2 Model Linking in OpenMI

The second stage in developing the multi-scale modelling framework involves linking the SPIDERR flow model with the ZOOMQ3D regional groundwater modelling code using OpenMI. In this linked composition, a radial flow model can quickly and easily be placed within a regional groundwater model, with the regional model providing a boundary condition for the smaller-scale model, as described below.

ZOOMQ3D is based on a finite difference approximation to the continuity equation, whereby specific discharge is calculated by Darcy's law (see equation 3). It incorporates local grid refinement, allowing problems to be solved across different scales on a Cartesian grid. As is the case for SPIDERR, ZOOMQ3D is able to represent multiple aquifer layers with varying hydraulic

parameters and confined and unconfined conditions. ZOOMQ3D also incorporates spatially and temporally varying recharge and river-aquifer interaction, and has been used to model several regional-scale aquifers in the UK for groundwater resource assessment purposes (Jackson et al., 2005; Jackson et al., 2011; Jones et al., 2012; Le Vine et al., 2016).

The OpenMI standard (Moore & Tindall, 2005; Gregersen et al., 2007) is a software component interface definition that can be used to link multiple different software components, including numerical models, databases, and analytical or visualization tools. When implemented, OpenMI compliant components can be configured to run simultaneously, exchanging data during computation. ZOOMQ3D was already OpenMI compliant, but the SPIDERR flow model (MATLAB) code had to be reconfigured into the structure required by OpenMI. This requires the solution algorithm, or model "engine", to be separated from code that initializes and terminates the simulation. This results in three principal program functions: (1) *Initialize*, which defines the set-up of the model; (2) *PerformTimeStep*, which solves the governing flow equation for a single time-step, and; (3) *Finish*, which writes output files and terminates the program. The restructured SPIDERR and ZOOMQ3D codes were each compiled as a dynamic-link library (dll); in the case of SPIDERR, the MATLAB compiler was used to compile the model as a C dll, including the MATLAB Compiler Runtime (MCR), allowing it to be deployed without a MATLAB licence. The OpenMI Software Development Kit (SDK) is used to write wrappers for the models, allowing the dlls to be accessed as OpenMI-compliant linkable components. OpenMI version 1.4 was used for this application and the OpenMI Graphical User Interface was used to link and run components. OpenMI provides functionality for linking multiple models, potentially allowing more than one axisymmetric model grid to be represented in a single regional model. Although this has not yet been implemented with SPIDERR and ZOOMQ3D, it would allow interaction between multiple boreholes to be simulated within a single regional-scale model.

The models are linked spatially by providing the location of the outer boundary of SPIDERR to ZOOMQ3D through the OpenMI interface. The Cartesian grids of the two models must be equivalent such that a single node on the SPIDERR model boundary links directly to a single node in ZOOMQ3D and, as mentioned above, the SPIDERR model currently only accommodates a square Cartesian mesh. This is achievable due to the local grid refinement capabilities of ZOOMQ3D. Due to the gridding requirements of SPIDERR, this also means that the location of the abstraction borehole in SPIDERR directly corresponds to a grid node in ZOOMQ3D, which is specified through the OpenMI interface. The layer elevations of the two models must be equivalent (SPIDERR can read these from the ZOOMQ3D input files), however layers can be vertically refined in SPIDERR to allow greater vertical resolution in the vicinity of the borehole. Consequently, a single ZOOMQ3D layer can be associated with multiple layers in SPIDERR. The linking of the models in this way relies on the assumption that flow across the boundary between ZOOMQ3D and SPIDERR is horizontal and Darcian.

The dynamic linking of the models is based on a one-way flow coupling, whereby ZOOMQ3D provides volumetric flows across the outer boundary of the SPIDERR Cartesian grid and provides recharge fluxes across the upper layer of SPIDERR. Under this one-way flow coupling, SPIDERR does not pass a boundary condition back to ZOOMQ3D; instead the regional model continues to perform calculations for the area occupied by the local model using equivalent parameters and stresses as SPIDERR to maintain consistency at the boundary between the two models. SPIDERR therefore passes the following variables to ZOOMQ3D at run-time through OpenMI: (1) the pumping rate at the borehole, which can be updated during a simulation based on the modelled groundwater head in the borehole by SPIDERR’s abstraction management module; (2) transmissivity and storage, which vary during a simulation based on fluctuation of

365 the water table. Table 1 provides more detail of the data exchange process between the two
366 models.
367

Exchanged Variables: ZOOMQ3D to SPIDERR	
Volumetric boundary flows	Passed directly from a ZOOMQ3D layer to the corresponding SPIDERR layer if no vertical refinement. If a ZOOMQ3D layer is refined in SPIDERR, boundary flows are partitioned and weighted according to the transmissivity of each layer at each time-step.
Lumped recharge fluxes	Including: recharge from rainfall, leakage to or from rivers or springs, additional point abstractions or discharges. Applied to the upper active layer in SPIDERR. Passed directly from ZOOMQ3D to the Cartesian grid of SPIDERR; partitioned across corresponding radial nodes in SPIDERR.
Exchanged Variables: SPIDERR to ZOOMQ3D	
Pumping rate at abstraction borehole	Passed directly from the abstraction borehole in SPIDERR to the corresponding abstraction node in ZOOMQ3D.
Model parameters	Including: horizontal and vertical hydraulic conductivity, specific storage and specific yield. With no vertical refinement in SPIDERR: • On the Cartesian grid of SPIDERR, parameter values are passed directly from SPIDERR to ZOOMQ3D • On the radial grid of SPIDERR, where multiple radial nodes are associated with a single ZOOMQ3D node, parameter values are averaged prior to being passed to ZOOMQ3D. With vertical refinement in SPIDERR:

	• Transmissivity (T) and storativity (S) of a single ZOOMQ3D layer is equal to the total T and S of all corresponding SPIDERR layers; • $K_{x,y}$ and Ss are calculated based on the total saturated thickness; • Sy (for unconfined layers) in ZOOMQ3D is taken from the uppermost corresponding layer in SPIDERR; • K_z in ZOOMQ3D is calculated as the weighted mean of K_z over all corresponding SPIDERR layers.

Table 1 Exchange items between SPIDERR and ZOOMQ3D when run as linked models through OpenMI

The exchange of data through the OpenMI interface at run-time is achieved using a pull-driven approach, which is based on a single linkable component being assigned as the driver of the multi-component composition. A function in OpenMI calls the driver component to update (i.e. proceed to the next time-step) at which point it requests all necessary data from all other linked components. This causes OpenMI to update the other linked components, which perform a time-step and provide data back to the driver so it can also proceed in time. If there is a two-way linkage between components, the driver provides an estimate of the required data based on the previous time-step so the second component can update and return the required computed values to the driver. Each linkable component provides a time-stamp at each time-step so the interface knows when all components have reached the same point in time. In this linked composition, in which SPIDERR is the driver, it is therefore possible for the two models to run at different temporal resolutions and over different time periods. SPIDERR, which uses adaptive time stepping, can run on a smaller time-step than ZOOMQ3D and data is transferred between the two models through OpenMI at the smallest common time-step. ZOOMQ3D will wait for SPIDERR to complete all sub time-steps, before both models proceed.

2.2 Model Evaluation

2.2.1 Radial-Cartesian Coupling

A vast number of grid configurations and model parameterisations could be run to evaluate the hybrid radial-Cartesian coupling method used in SPIDERR. In this case, the model was evaluated against the Papadopulos-Cooper solution for simulating drawdown in a large diameter well in a confined aquifer (Papadopulos & Cooper, 1967). Several grid configurations were set up to analyse model error related to the radial-Cartesian boundary in SPIDERR for different levels of radial and Cartesian grid refinement (Table 2 and Figure 3). The results presented here are in no way exhaustive, and many more grid configurations could be tested. The results presented below help to illustrate the value and limitations of the methodology but further testing of different grid configurations under different aquifer conditions (e.g. unconfined, vertically heterogeneous, or non-Darcian flow) would be valuable.

SPIDERR was run as a single layer, homogeneous, confined model with a 0.1m diameter borehole located at the center of a 20 $\times$ 20 km Cartesian grid. The model was run over a period of 50 days with an abstraction rate of 1000 m^3day^{-1}, a transmissivity of 500 m^2day^{-1} and a storativity of 0.005. Three different Cartesian grids were used, with square cells 250, 500, and 1500 m wide. In each of these, three different radial grids were also applied containing 4, 12 or 20 radial slices, which have different radial extents as shown in Figure 3. Simulated drawdown at the abstraction borehole and at the node in the central-slice on the radial-Cartesian boundary was compared with the analytical solution (Figure 4). The percentage error, calculated at the end of the simulation from drawdown at the abstraction borehole and drawdown at the central-slice node on the radial-Cartesian boundary, is shown in Table 2.

The results show that a four-slice radial model produces relatively high errors at the boundary, which are also visible at the abstraction borehole. The timing of the deviation from the analytical solution at the borehole varies with the extent of the radial grid, with the effects of the boundary seen earliest in the four radial slice / 250 m Cartesian set-up as the boundary is closest to the borehole in this configuration. Refinement on the Cartesian grid generally improves the error at the boundary and has a small impact on the error at the borehole. Errors in simulated drawdown are significantly reduced by increasing the resolution on the radial grid from four to 12 radial slices (see Table 2). For the 12-slice model, errors are slightly higher at the corner boundary nodes because the cell area is larger, therefore the assumption of uniform head across the cell is less valid. Table 2 suggests that increasing the radial refinement from 12 to 20 slices appears to increase the error at the boundary; however, the 20-slice model has a larger radial extent than the 12-slice model with the same number of radial nodes, therefore a coarser resolution at the boundary so the configurations are not directly comparable. For each of the validation runs shown in Table 2 and Figure 4 the model was set-up with 40 nodes along the radial dimension. For the 20-slice radial model with a 1500 m Cartesian grid resolution, the error at the boundary and abstraction borehole can be reduced further to 2.29% and 0.05%, respectively, by increasing the number of radial nodes from 40 to 80.

The boundary errors are dependent on an interplay between refinement on the Cartesian and radial grids however, the validation results indicate that errors related to the coupling methodology are most sensitive to the number of radial slices in the SPIDERR model with an increase from four to 12 slices providing the greatest reduction in error. As mentioned above, further testing of different grid configurations for specific model and aquifer setups would be recommended.

Test	Cartesian Grid Resolution (m)	Number Radial Slices	Radial Boundary Extent (m)	Error at the abstraction borehole (%)	Boundary Error for Central Slice (%)
1	250	4	125	2.23	6.27
2	250	12	375	0.07	0.25
3	250	20	625	0.27	1.33
4	500	4	250	2.23	8.03
5	500	12	750	0.03	0.06
6	500	20	1250	0.18	1.96
7	1500	4	750	2.24	14.1
8	1500	12	2250	0.18	2.14
9	1500	20	3750	0.16	6.95

434 *Table 2 Grid configurations to evaluate SPIDERR model error*

435

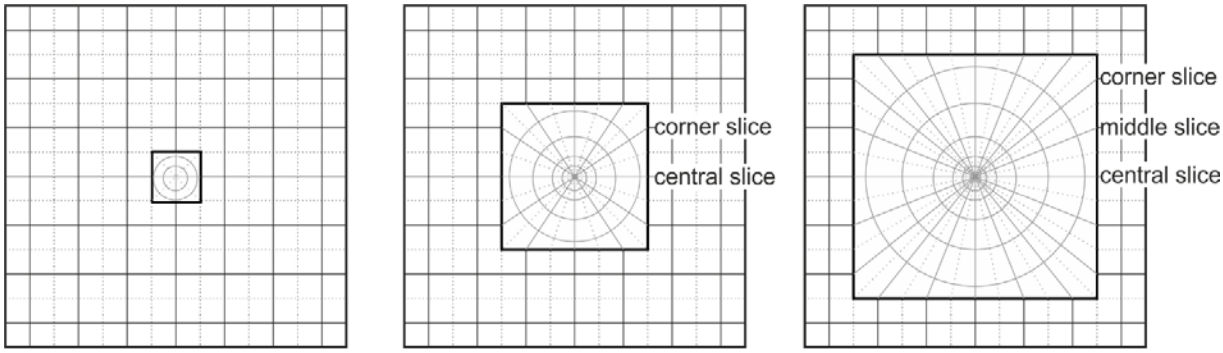

436 (a) (b) (c)

437 *Figure 3 Grid configurations for SPIDERR validation: (a) 4 slice radial model; (b) 12-slice radial model; (c)*

438 *20-slice radial model.*

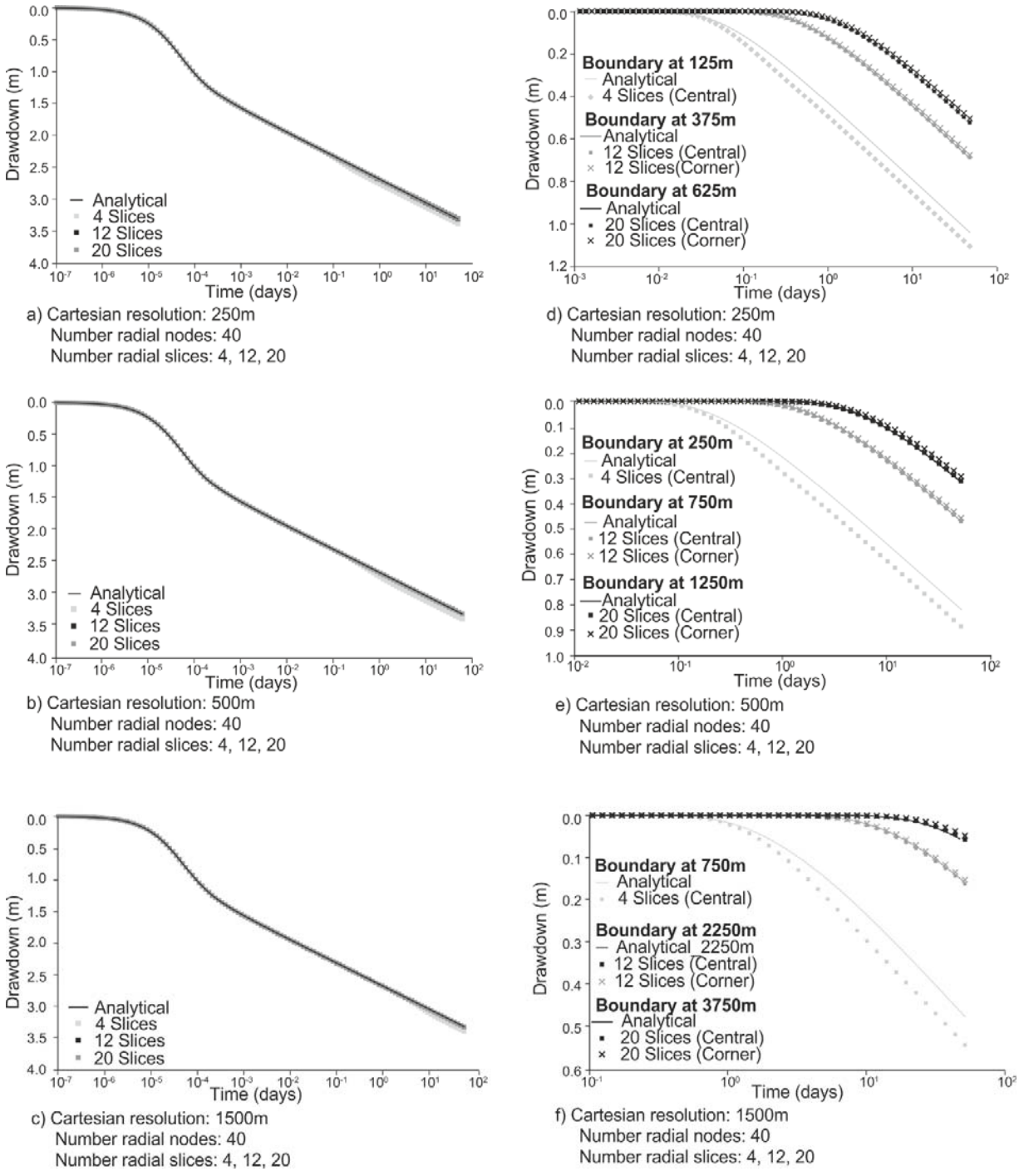

Figure 4 Simulated drawdown compared with the Papadopulos-Cooper solution at the abstraction borehole (a-c) and on the radial-Cartesian boundary (d-f) for different levels of radial and Cartesian grid refinement.

2.2.2 Model Linking in OpenMI

The method for linking SPIDERR and ZOOMQ3D through OpenMI was evaluated by comparing a standalone SPIDERR model, standalone ZOOMQ3D model, and coupled composition for an aquifer of increasing complexity. The standalone SPIDERR model was set up as for Test 2 above (i.e. a 12 slice radial grid with a radial extent of 375m, coupled to a 20 × 20 km Cartesian grid at a resolution of 250 m). The standalone ZOOMQ3D model had an equivalent Cartesian grid with an abstraction node located at its center. The standalone models were initially compared for the series of aquifers outlined in Table 3. For each simulation the models were run over a period of 50 days on a daily time-step with a constant abstraction rate of 1000 m^3/day. In simulations four and five, vertical heterogeneity and anisotropy were introduced in the multi-layer SPIDERR models by varying horizontal hydraulic conductivity (Kh) with depth and reducing vertical hydraulic conductivity (Kv) relative to Kh (Table 3). ZOOMQ3D was kept as a single-layer homogeneous model. Specific storage and specific yield (for the unconfined simulations) were kept constant at 2.5 x 10^{-4} m^{-1}, and 0.1, respectively, in both models.

		SPIDERR				**ZOOMQ3D**		
Simulation	**Aquifer Type**	**Nbr Layers**	**Layer Thickness (m)**	**Kh (m/d)**	**Kv (m/d)**	**Nbr Layers**	**Layer Thickness (m)**	**Kh (m/d)**
1	Confined	1	20	25	-	1	20	25
2	Unconfined	1	20	25	-	1	20	25
3	Unconfined	3	4 6 10	25 25 25	25 25 25	1	20	25
4	Unconfined	3	4	100	25	1	20	25

			6 10	12.5 2.5	25 25			
5	Unconfined	3	4 6 10	100 12.5 2.5	0.25 0.25 0.25	1	20	25

Table 3 Model setup for evaluation of the SPIDERR-ZOOMQ3D coupling methodology

Comparison of the standalone SPIDERR and ZOOMQ3D models shows that the inconsistencies between the two models, related to the more detailed discretization of the borehole and aquifer in SPIDERR, are relatively local to the borehole. As would be expected, ZOOMQ3D is unable to reproduce drawdown at the borehole itself, which is represented in the regional model as a single Cartesian node with dimensions of 250 × 250 m (Figure 5a). Discretization errors can also be seen at a distance of 500 m from the borehole in ZOOMQ3D, and these errors are more significant in the unconfined simulations (Figure 5b). However, at a distance of 1000 m from the borehole the two standalone models are largely consistent, even where significant vertical heterogeneity and anisotropy are introduced in the unconfined multi-layer SPIDERR model. Increasing anisotropy causes larger vertical hydraulic gradients to develop in the aquifer, but again these are local to the borehole (Figure 6). For these simulations vertical hydraulic gradients, and thus vertical flow, are reduced to zero at the boundary of the radial grid within the SPIDERR model, satisfying the assumption of horizontal flow for linking with ZOOMQ3D.

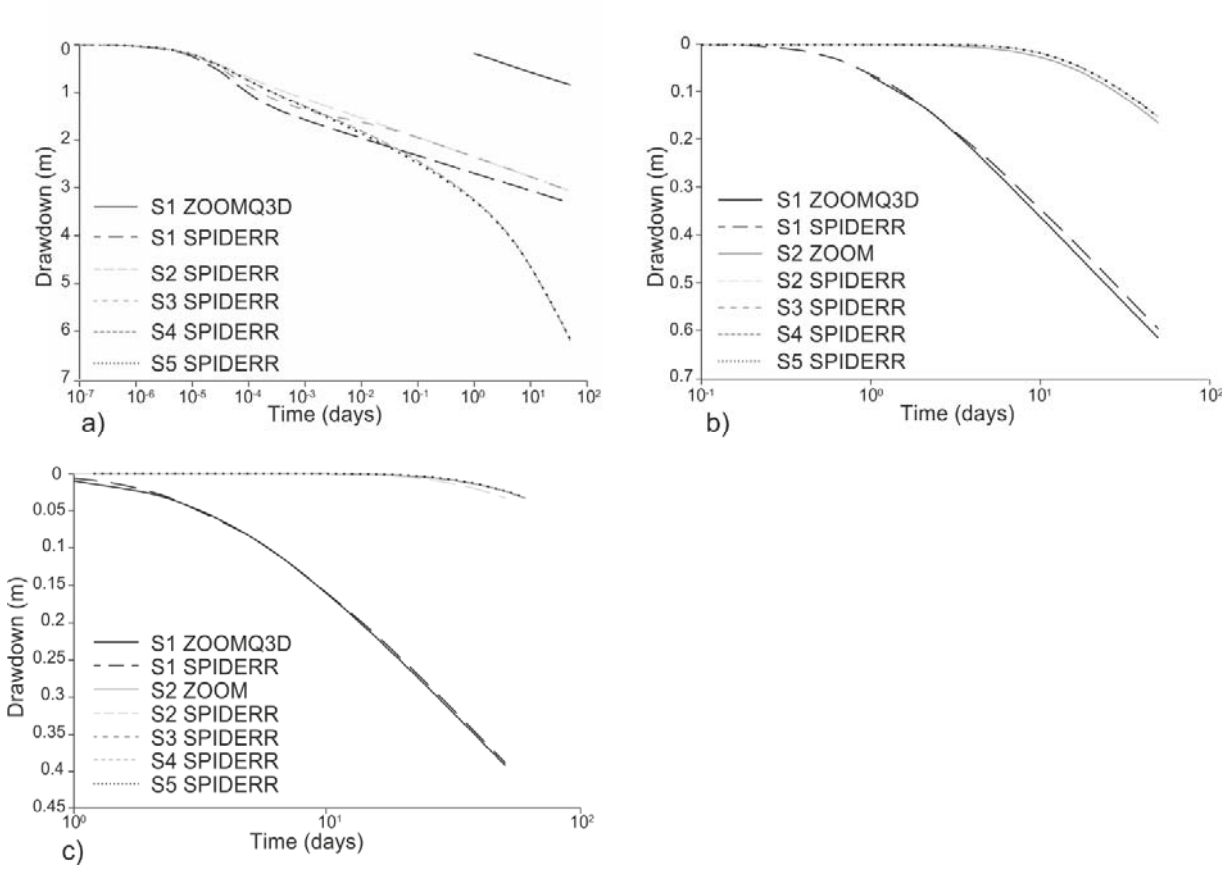

Figure 5 Simulated drawdown in standalone SPIDERR and ZOOMQ3D models for simulations 1-5, as outlined in Table 3, at: (a) the abstraction borehole; (b) 500m from the borehole; (c) 1000m from the borehole

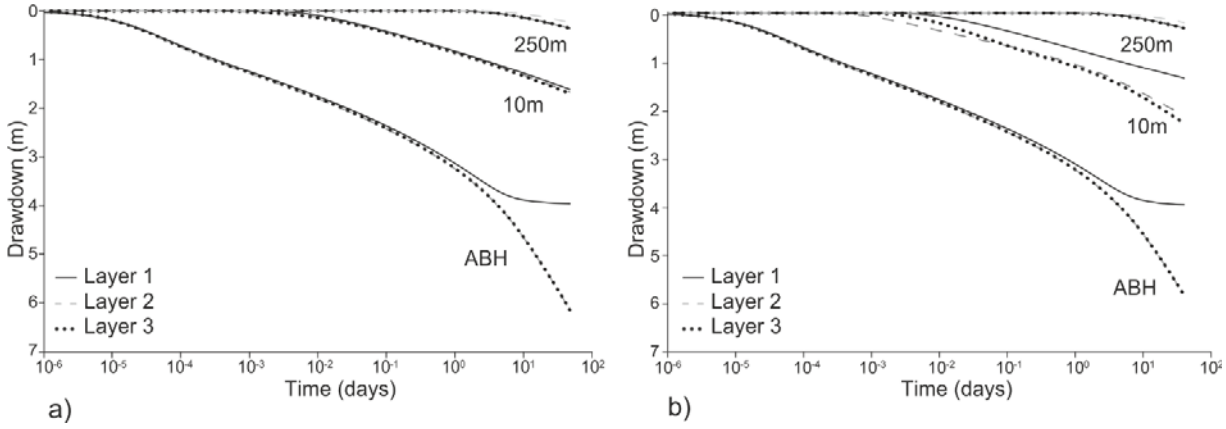

Figure 6 Simulated drawdown in each layer (Layer 1, 2 and 3) of the standalone SPIDERR model at the borehole (ABH) and at 10 m and 250 m from the ABH for (a) simulation 4; (b) simulation 5.

A linked composition was set up for simulation 5. This used a SPIDERR model covering a 1500 × 1500 m area with a 250 m resolution Cartesian grid and 12-slice radial grid. The results of the standalone simulations indicated that at this SPIDERR model boundary (i.e. a radial distance of 750 m from the borehole) the two models were consistent and flow in the multi-layer SPIDERR model was horizontal. The SPIDERR model was therefore linked to the 20 × 20 km ZOOMQ3D grid through OpenMI and the models were run over the same 50-day time period, exchanging data on a daily time-step. The results of this simulation are compared with the equivalent standalone SPIDERR model at various points on the radial and Cartesian grids, showing good agreement (Figure 7). In this coupled simulation, the abstracted volume is initially derived from well storage, before water is released from storage on the radial grid. The cone of depression reaches the boundary of the radial SPIDERR grid after approximately one day, at which point the Cartesian grid starts to provide water to the borehole. After six days, flow across the SPIDERR model boundary increases, with ZOOMQ3D contributing just under one third of the total abstraction rate by the end of the simulation.

As discussed in Section 2.2.1, there are a vast number of model set-ups that could be run to evaluate the methodology. The results presented here show that the linked composition reproduces the standalone SPIDERR model results even when a significant amount of flow is passed across the ZOOMQ3D-SPIDERR boundary and the SPIDERR model is vertically refined compared with the regional model. This indicates that the methodology is valid for representing the refined area around a borehole within a regional groundwater model. However, further evaluation could be undertaken to test the methodology under different aquifer conditions.

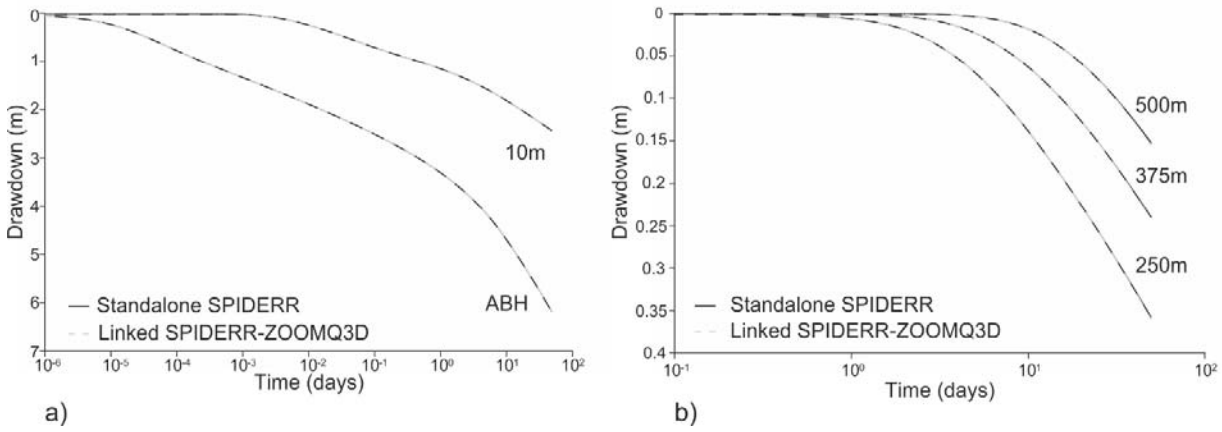

Figure 7 Comparison of standalone SPIDERR and linked SPIDERR-ZOOMQ3D simulations for simulation 5 (i.e. refined, heterogeneous, and anisotropic SPIDERR model) at: (a) the abstraction borehole and 10 m distance from the abstraction borehole; (b) 250m and 375m from the borehole on the radial grid, and 500m from the abstraction borehole on the Cartesian grid.

3. MODEL APPLICATION

To further evaluate the methodology, the linked modelling framework was applied to a public water supply borehole (Borehole A) located in the River Thames catchment in southern England. This groundwater source was chosen for evaluation purposes as it is a relatively simple single-borehole source, for which pumping test and operational data are available, and it is located within an existing regional groundwater model, described below, that has been widely used for groundwater resource assessment.

3.1 Study Area

The exact location of Borehole A, which is operated by Thames Water Utilities Ltd., cannot be given for confidentiality reasons but is situated in the Chalk aquifer – a principal aquifer in the UK, accounting for up to 70% of the total public water supply in parts of southern England (Allen et al., 1997; Butler et al., 2012). The Chalk is a very fine-grained limestone with a low permeability matrix and highly permeable fracture network, which is often enhanced by

dissolution and provides the main mechanism for groundwater flow in the aquifer (Allen et al., 1997; MacDonald, 1998). Vertical and lateral variations in transmissivity and storativity are controlled by fracture development in the Chalk, which is greater at shallow depths and in valleys and dry valleys. Transmissivity estimates from pumping test data range from 50 m^2day^{-1} in interfluvial areas to 500-2000 m^2day^{-1} in valleys and dry valleys. These variations have a strong influence on the yield of abstraction boreholes, which often decrease non-linearly as groundwater levels fall (Williams et al., 2006; Butler et al., 2009). Borehole A is drilled to a depth of 55 m into the unconfined Chalk aquifer, penetrating the Lewes Nodular and underlying New Pit Chalk Formations (Mortimore, 1986; Robinson, 1986). The Lewes Nodular Chalk has a higher flint content than the underlying New Pit Chalk and an important hard band, the Chalk Rock, marks the boundary between the formations. Geophysical logging of the borehole indicates that more than 75% of the total inflow occurs within the upper 32 m of the borehole (i.e. from the Lewes Nodular Chalk), with significant inflows at depths of 22 m and 32 m associated with fracturing and the Chalk Rock, respectively. Borehole A is located within the valley of the River Kennet, a major tributary of the River Thames. Groundwater level data from observation boreholes near Borehole A show relatively small fluctuations and shallow hydraulic gradients, indicative of a highly transmissive groundwater system. This was confirmed by a Jacob straight line analysis of a five-day constant rate pumping test at Borehole A, which gave transmissivity estimates of more than 2000 m^2day^{-1}. Borehole A is licensed to abstract at an average rate of 2500 m^3day^{-1}.

3.2 Model Setup

3.2.1 ZOOMQ3D Regional Groundwater Model

Borehole A is located within the ZOOMQ3D regional groundwater model of the Marlborough and Berkshire Downs. This model is described in detail by Jackson et al. (2011; 2015). The

existing regional groundwater model had a variable mesh resolution of between 100 m and 2 km, but only covered the area of Borehole A at the coarsest resolution. Consequently the grid was refined to 500 m over the River Kennet catchment and then to 250 m around Borehole A. This allowed greater accuracy in the positioning of the abstraction borehole in the regional model and a more detailed representation of the River Kennet, which is approximately 500 m from the borehole. The regional groundwater system is represented in the model by three layers, which were informed by 3D geological modelling of the lithostratigraphy of the Chalk group. In the vicinity of Borehole A, the model layers correspond well to the geophysical logs of the borehole, with Layer 1 representing the Lewes Nodular Chalk Formation and Chalk Rock, which contribute the majority of inflow, and Layer 2 representing the New Pit Chalk Formation, the base of which is 5 m below the base of the borehole. Comparison of modelled and observed groundwater levels from the nearest observation borehole, located 1.7 km from Borehole A, showed good agreement (Figure 8). No further development or calibration of the regional groundwater model were therefore undertaken for this study.

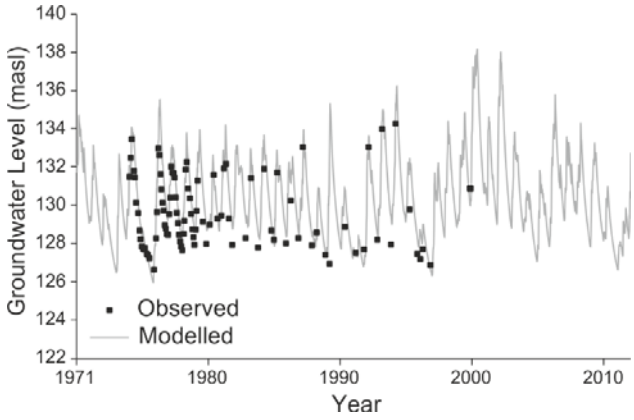

Figure 8 Modelled and observed groundwater levels at closest observation borehole to Borehole A.

3.2.2 SPIDERR

The SPIDERR flow model was initially calibrated as a standalone model to the five-day constant rate pumping test data from Borehole A. This first model had a 10 km radius, a 0.96 m diameter

open borehole at its center and an outer fixed head boundary. The radial dimension was discretized using 51 nodes spaced logarithmically between the borehole and outer boundary, the circumferential dimension was split into 12 slices, and the vertical dimension was represented as three layers using the layer elevations from the regional groundwater model. The borehole was extended to the bottom of layer 2 and was pumped using the abstraction rates shown in Figure 8. These do not incorporate the early-time fluctuations in abstraction rate pumping, which were related to issues with the electricity generator running the borehole pump.

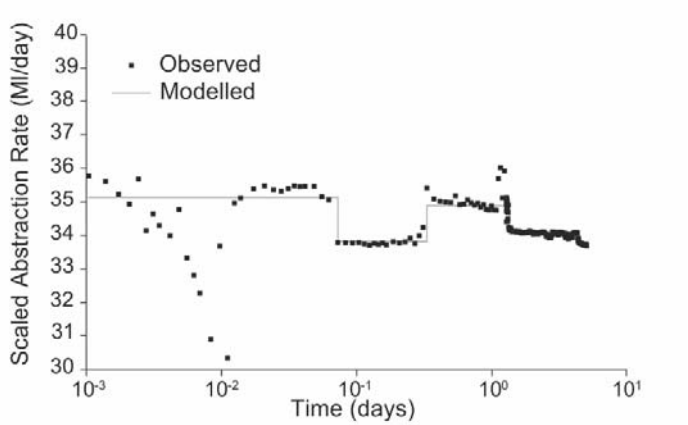

Figure 9 Observed and modelled abstraction rates for the five-day constant rate pumping test at Borehole A. Abstraction rates have been scaled for confidentiality reasons. Data provided courtesy of Thames Water Utilities Limited.

An initial model run (SFM Run 1) was undertaken using the regional model parameters in the vicinity of Borehole A, which were then calibrated to observed groundwater levels from the abstraction borehole and a nearby observation borehole located 15 m away. The calibration process was informed by a brief sensitivity analysis, which indicated the model results were most sensitive to the hydraulic conductivity and Forchheimer parameter in layer 1. All other parameters were therefore kept constant and these two parameters were adjusted to fit the observed groundwater levels in the abstraction and observation borehole. The results of the final calibration (SFM Run 4) are shown in Table 4 and Figure 10. The transmissivity of the fully

saturated model from SFM Run 4 is just under 2000 m^2 day^{-1}, which is close to the value derived from the Jacob straight-line analysis of the constant rate test data.

	$K_h(1)$ m day^{-1}	$K_h(2)$ m day^{-1}	$K_h(3)$ m day^{-1}	$S_y(1)$ -	$S_s(1\text{-}3)$ m^{-1}	$\beta(1)$ m^{-1} day
Regional model parameters (SFM Run 1)	58	19	1	0.03	5×10^{-7}	0
Calibrated parameters (SFM Run 4)	76	19	1	0.03	5×10^{-7}	0.075

Table 4 Initial and calibrated parameters of the standalone SPIDERR Flow Model

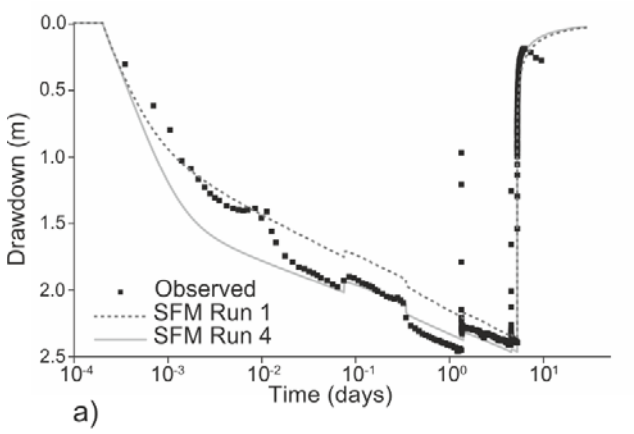

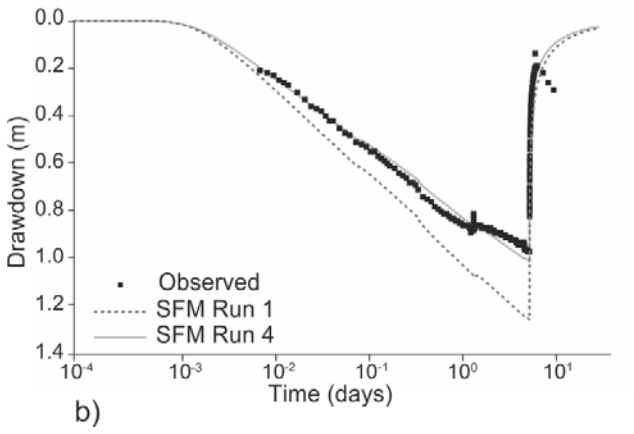

Figure 10 Observed and modelled drawdown in Borehole A during the five-day constant rate pumping test: (a) at the abstraction borehole; (b) at the observation borehole. Observed data provided courtesy of Thames Water Utilities Limited.

3.2.3 Coupled Model

The SPIDERR model was coupled with the ZOOMQ3D regional model as shown in Figure 11. Borehole A sits at the center of the SPIDERR grid and corresponds to a single node in the regional model. Around the abstraction borehole, the regional model and Cartesian grid of the SPIDERR model have a resolution of 250 m and the SPIDERR grid extends over an area of 1500 $\times$ 1500 m. Nine Cartesian nodes of the SPIDERR grid are replaced by a 12 slice radial model with a radius of 375 m. The three vertical layers are equivalent in the two models. The parameters from the calibrated standalone radial model (Table 4) are applied in the SPIDERR model and transferred to ZOOMQ3D through the OpenMI linking process, updating the parameters of the regional model within the boundary of the local-scale model. The coupled model is run through OpenMI on a daily time-step over the historic simulation period 1971 to 2012. Daily abstraction rates are available for Borehole A from 2003, when it first became operational. Weekly abstraction rates are available for a decommissioned borehole located 15 m from Borehole A (now used as an observation borehole) from 1971 to 2003. The two abstraction data sets are combined into a weekly time-series (shown from 2003-2012 in Figure 12) and applied at Borehole A in the SPIDERR model. Abstraction rates are passed from SPIDERR to the borehole node in ZOOMQ3D through the linking process in OpenMI, which also transfers the following daily volumetric data from the regional model to the local-scale model: flows across the SPIDERR boundary, distributed recharge, and leakage between the river and aquifer nodes along the River Kennet.

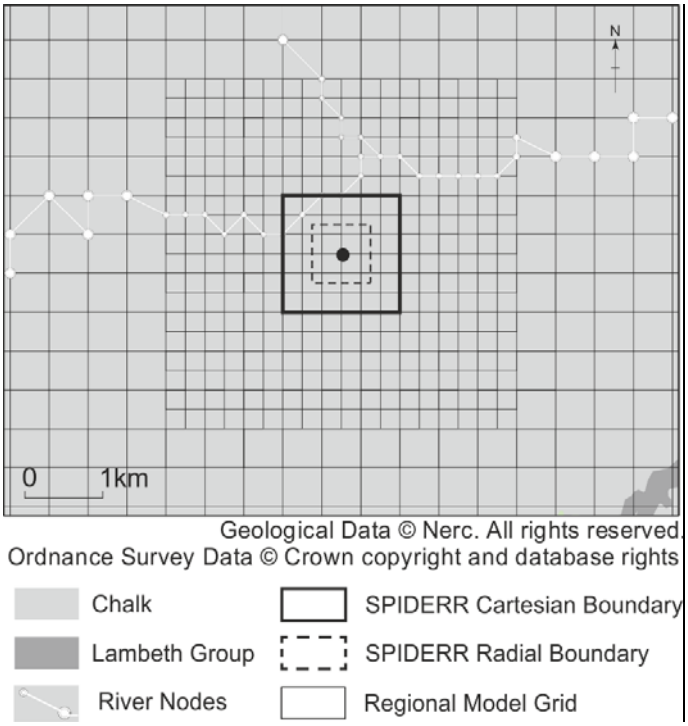

Figure 11 Coupled model composition around Borehole A

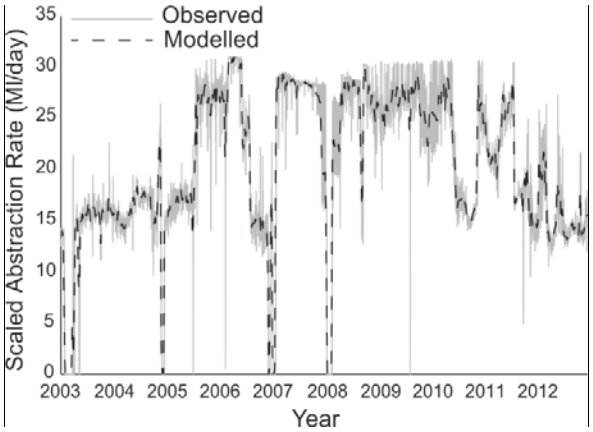

Figure 12 Operational (observed) and modelled abstraction rates over the simulation period. Abstraction rates have been scaled for confidentiality reasons. Observed data provided courtesy of Thames Water Utilities Limited.

3.3 Results

The results of the linked simulation are compared with groundwater levels monitored in Borehole A, which were available from 2008-2012 (Figure 13a). Simulated groundwater levels are also compared with observed levels from the decommissioned borehole, which was monitored over the period 2003-2006 (Figure 13b). Figure 13a shows very good agreement between modelled and operational water levels within the abstraction borehole. Daily or sub-daily fluctuations related to abstraction are not represented due to use of the weekly averaged abstraction rates, however these are generally small compared with the seasonal fluctuations, which are reproduced well by the model. In the observation borehole, simulated groundwater levels match the average observed groundwater level but show a greater degree of fluctuation than the observed time-series. This is most likely due to storage in the decommissioned borehole, which has a large diameter of 2.7 m and is represented in the model as a normal aquifer node with a specific yield of only 0.03, but this could be explored further through a sensitivity analysis.

Consistency between the two models, thus accuracy of flows passed from the regional- to the local-scale model, was evaluated by comparing simulated groundwater levels at equivalent points on the Cartesian grids in SPIDERR and ZOOMQ3D. The difference between groundwater levels in the two models was less than 0.1 m at all locations, providing confidence in the coupling procedure. Furthermore, the additional computational burden associated with the coupled composition was not prohibitive. The standalone regional model, which consists of 3118 grid nodes, required a run-time of 518 minutes while the coupled composition, which contains an additional 1299 computational nodes, required 862 minutes to run. The increased run-time was therefore proportional to the increased number of nodes in the coupled

composition, which allows significant refinement around the abstraction borehole compared to the standalone regional model.

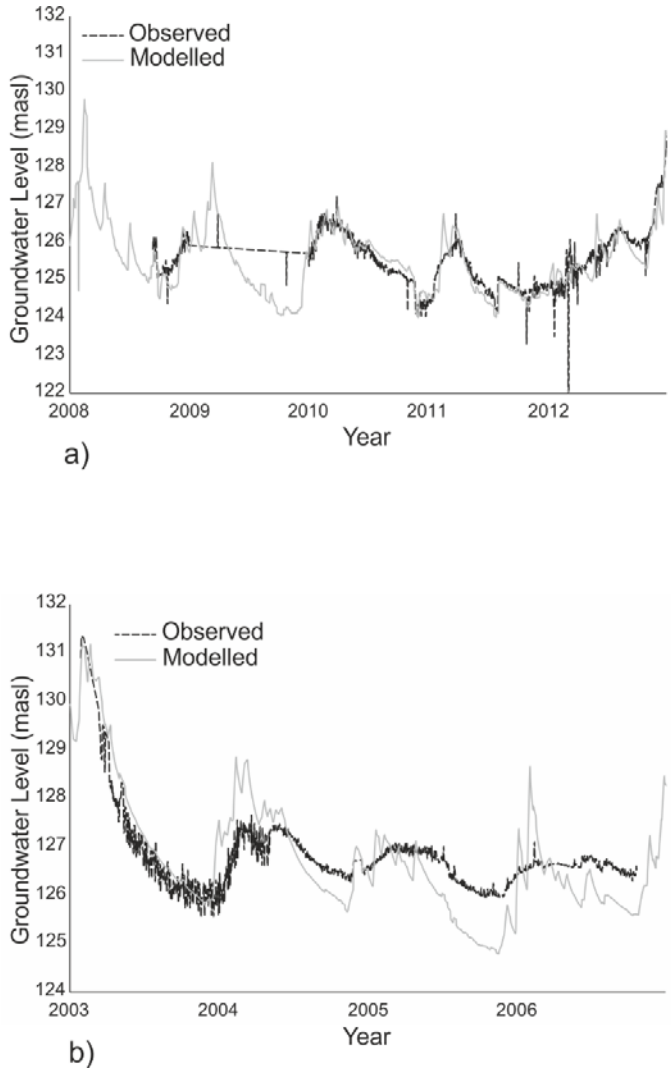

Figure 13 Simulated and observed groundwater levels at (a) the abstraction borehole (Borehole A), and (b) the decommissioned borehole located 15 m from Borehole A. Observed data provided courtesy of Thames Water Utilities Limited.

4. DISCUSSION

The SPIDERR flow model has previously been shown to reproduce drawdown in complex heterogeneous aquifers through application to a borehole in a fractured chalk aquifer, which

displays vertical heterogeneity (in both the borehole and aquifer) and non-Darcian flow (Upton et al., 2019). The hybrid radial-Cartesian model developed and applied in this study allows the borehole-scale model to be linked with a regional-scale groundwater model through OpenMI. While there have been recent advancements in multi-scale groundwater modelling that allow groundwater processes to be simulated across multiple scales, such as MODFLOW-USG (Panday et al., 2017), this methodology provides a novel way of simultaneously representing regional and local-scale groundwater processes. Unlike existing models, it allows a much more detailed representation of the borehole-scale processes and features, including non-Darcian flow, which can significantly impact drawdown and borehole yields, particularly in fractured aquifers.

The key limitations of the methodology are related to errors across the radial-Cartesian boundary and SPIDERR-ZOOMQ3D boundary; however evaluation against analytical solutions and a standalone radial flow model show that these errors can be minimized with appropriate grid refinement and construction, which is made easy by the two model codes. Errors across the radial-Cartesian boundary within SPIDERR are particularly minimized by refinement in the circumferential direction, with a 12-slice radial model providing the optimum grid set-up. Refinement on the Cartesian grid and along the radial dimension of the radial grid were found to have less influence on the accuracy of the solution in SPIDERR. Linking SPIDERR with ZOOMQ3D through OpenMI requires the two models to be equivalent at the grid boundary and is based on the assumption that flow is largely horizontal and Darcian. These requirements can be met by positioning the boundary of the SPIDERR model at an appropriate distance from the abstraction borehole such that the effects of non-Darcian flow and vertical head gradients due to drawdown around the borehole are negligible, and discretization errors related to the representation of the abstraction borehole in ZOOMQ3D are also negligible. This will be site-

specific, but test simulations indicate that the effects of vertical heterogeneity and anisotropy may be fairly local (e.g. << 250 m, see Figure 6) to the abstraction borehole. The extent of the SPIDERR model in a linked composition can be determined by test simulations using standalone models, or through calculation of the approximate extent of the cone of depression of the borehole from long-term average abstraction and recharge.

While the methodology presented here provides less flexibility in grid construction compared with other multi-scale methods, such as the control-volume finite difference or finite element method, the simplicity of this method ensures it is very user-friendly and efficient to solve. The use of OpenMI to link the two models means that a standalone radial flow model can be developed and calibrated to an individual abstraction borehole, ideally through the use of pumping test data, prior to coupling with a regional model. This is easier than trying to calibrate a small area of interest in a regional-scale model, particularly if the method is to be applied to multiple sources. It also makes the solution process more efficient as individual sources can effectively be switched on and off in the regional model when they are not required. The methodology allows existing groundwater models, which often represent significant investments, to be used without any complicated or time-consuming changes to the grid structure and the multi-scale groundwater model can be quickly and easily linked with other OpenMI compliant codes for water resources management. This has already been done by Foster et al. (2017), who used a linked SPIDERR-ZOOMQ3D composition to investigate the impacts of well yield on irrigation economics.

The application of the methodology to a relatively simple single-source abstraction site in the Chalk aquifer of southern England demonstrates the ability of the model to reproduce the operational groundwater level time-series in a supply borehole. Further evaluation of the

methodology will require application to more complex abstraction sites with, for example, greater degrees of aquifer heterogeneity or multiple boreholes. The potential for linking multiple borehole models with a single regional groundwater model provides an opportunity to investigate interference effects between neighbouring abstraction boreholes, and impacts of multiple groundwater abstractions on other parts of the environment, e.g. rivers or wetlands. The linked methodology also provides the opportunity to run predictive scenarios to investigate the potential impacts of climate change or increasing demand on the sustainable yield of supply boreholes, which is a critical part of water resource management, particularly for strategically important aquifers, or those vulnerable to over-exploitation.

5. CONCLUSIONS

The linked modelling methodology presented in this paper provides a tool for effective groundwater resources management, whereby groundwater sources can be simulated within their regional context to enable short- and long-term groundwater availability to be assessed at the scale of the individual abstraction borehole and wider aquifer. The methodology links a borehole-scale non-linear radial flow model – SPIDERR (Upton et al., 2019) – to ZOOMQ3D, a regional groundwater modelling code, using OpenMI. SPIDERR represents the small-scale features and processes required to simulate the groundwater level in a pumped borehole, including features of the borehole itself, aquifer heterogeneity, and non-Darcian flow (Upton et al., 2019), while ZOOMQ3D represents the regional processes that can also influence the sustainable yield of an abstraction borehole, including large-scale aquifer heterogeneity, distributed recharge and discharge to rivers and springs. The methodology is shown to reproduce operational groundwater levels at a supply borehole in the Chalk aquifer in the UK, and has many potential applications for both water resource management and environmental

management more widely, particularly in the context of climate change in increasing global demand for water.

6. ACKNOWLEDGEMENTS

The linked model was jointly developed by Imperial College London (ICL) and the British Geological Survey (BGS) and is jointly owned by ICL and BGS. This work was funded under an Engineering and Physical Sciences Research Council (EPSRC) doctoral training programme grant (EP/P505550/1). Additional support was provided through core Natural Environment Research Council funds of the British Geological Survey (BGS), and by Thames Water Utilities Limited (TWUL). Pumping test data were also provided by TWUL and invaluable advice on the source and test data was provided by Mike Jones and Jamie Riches (TWUL). Upton and Jackson publish with the permission of the Executive Director of the BGS.

7. REFERENCES

Aavatsmark, I. (2002). "An introduction to multipoint flux approximations for quadrilateral grids." Computational Geosciences **6**(3-4): 405-432.

Aavatsmark, I., et al. (1996). "Discretization on non-orthogonal, quadrilateral grids for inhomogeneous, anisotropic media." Journal of Computational Physics **127**(1): 2-14.

Abrams, D. B., et al. (2016). "Field Test of a Hybrid Finite-Difference and Analytic Element Regional Model." Groundwater **54**(1): 66-73.

Akbar, A. M., Arnold, M.D, Harvey, A.H (1974). Numerical Simulation of Individual Wells in a Field Simulation Model SPE 4073. SPE-AIME 47th Annual Fall Meeting. San Antonio, Texas, American Institute of Mining, Metallurgical, and Petroleum Engineers.

Al-Salamah, I. S., et al. (2011). "Groundwater modeling of Saq Aquifer Buraydah Al Qassim for better water management strategies." Environmental Monitoring and Assessment **173**(1-4): 851-860.

Allen, D. J., et al. (1997). The physical properties of major aquifers in England and Wales, British Geological Survey Technical Report, WD/97/34.

Anwar, S., et al. (2008). "Lattice Boltzmann simulation of solute transport in heterogeneous porous media with conduits to estimate macroscopic continuous time random walk model parameters." Progress in Computational Fluid Dynamics **8**(1-4): 213-221.

Anwar, S. and M. C. Sukop (2009a). "Lattice Boltzmann Models for Flow and Transport in Saturated Karst." Ground Water **47**(3): 401-413.

Anwar, S. and M. C. Sukop (2009b). "Regional scale transient groundwater flow modeling using Lattice Boltzmann methods." Computers & Mathematics with Applications **58**(5): 1015-1023.

Bandilla, K. W., et al. (2009). "A parallel mesh-free contaminant transport model based on the Analytic Element and Streamline Methods." Advances in Water Resources **32**(8): 1143-1153.

Betrie, G. D., et al. (2011). "LINKING SWAT AND SOBEK USING OPEN MODELING INTERFACE (OPENMI) FOR SEDIMENT TRANSPORT SIMULATION IN THE BLUE NILE RIVER BASIN." Transactions of the Asabe **54**(5): 1749-1757.

Butler, A. P., et al. (2012). Advances in modelling groundwater behaviour in Chalk catchments. Groundwater Resources Modelling: A Case Study from the UK. M. G. Shepley, M. I. Whiteman, P. J. Hulme and M. W. Grout, Geological Society London, Special Publications, 364**:** 113-127.

Butler, A. P., et al. (2009). "Analysis of flow processes in fractured chalk under pumped and ambient conditions (UK)." Hydrogeology Journal **17**(8): 1849-1858.

Butts, M., et al. (2013). Embedding complex hydrology in the climate system - towards fully coupled climate-hydrology models. Climate and Land Surface Changes in Hydrology. E. Boegh, E. Blyth, D. M. Hannah et al. Wallingford, Int Assoc Hydrological Sciences. **359:** 133-139.

Castronova, A. M. and J. L. Goodall (2013). "Simulating watersheds using loosely integrated model components: Evaluation of computational scaling using OpenMI." Environmental Modelling & Software **39**: 304-313.

Castronova, A. M., et al. (2013). "Integrated modeling within a Hydrologic Information System: An OpenMI based approach." Environmental Modelling & Software **39**: 263-273.

Chen, C. S., et al. (2003). "An unstructured grid, finite-volume, three-dimensional, primitive equations ocean model: Application to coastal ocean and estuaries." Journal of Atmospheric and Oceanic Technology **20**(1): 159-186.

Connorton, B. J. and R. N. Reed (1978). "A numerical model for the prediction of long term well yield in an unconfined chalk aquifer." Quarterly Journal of Engineering Geology and Hydrogeology **11**(2): 127-138.

Diersch, H.-J. G. (2002). FEFLOW - Reference Manual. Berlin, DHI-WASY GmbH.

Ding, Y. and L. Jeannin (2001). New Numerical Schemes for the Near-Well Modelling with Discretization Around the Wellbore Boundary Using Flexible Grids (SPE 66360). SPE Reservoir Simulation Symposium. Houston, Texas, Society of Petroleum Engineers.

Ebraheem, A. M., et al. (2004). "A local-scale groundwater flow model for groundwater resources management in Dakhla Oasis, SW Egypt." Hydrogeology Journal **12**(6): 714-722.

Eissa, M. A., et al. (2013). "Groundwater resource sustainability in the Wadi Watir delta, Gulf of Aqaba, Sinai, Egypt." Hydrogeology Journal **21**(8): 1833-1851.

Elag, M. M., et al. (2011). "Feedback loops and temporal misalignment in component-based hydrologic modeling." Water Resources Research **47**.

Feinstein, D. T., et al. (2016). "A Semi-Structured MODFLOW-USG Model to Evaluate Local Water Sources to Wells for Decision Support." Groundwater **54**(4): 532-544.

Foster, T., et al. (2017). "Effects of initial aquifer conditions on economic benefits from groundwater conservation." Water Resources Research **53**(1): 744-762.

Fung, L. S. K., Buchanan, L., Sharma, R. (1994). "Hybrid-CVFE Method for Flexible-Grid Reservoir Simulation." SPE Reservoir Engineering(August 1994): 188-194.

Gleeson, T., et al. (2012). "Water balance of global aquifers revealed by groundwater footprint." Nature **488**(7410): 197-200.

Goodall, J. L., et al. (2013). "Coupling climate and hydrological models: Interoperability through Web Services." Environmental Modelling & Software **46**: 250-259.

Gottardi, G., Vignati, L. (1990). "Hybrid Grid Black Oil Reservoir Simulator." Journal of Petroleum Science and Engineering **3**: 345-360.

Gregersen, J. B., et al. (2007). "OpenMI: Open modelling interface." Journal of Hydroinformatics **9**(3): 175-191.

Heinemann, Z. E., Brand, C.W, Munka, M., Chen, Y.M (1991). "Modelling Reservoir Geometry with Irregular Grids." SPE Reservoir Engineering(May 1991): 225-232.

Hiebert, A. D., et al. (1993). "COMPARISON OF DISCRETIZATION METHODS FOR MODELING NEAR-WELL PHENOMENA IN THERMAL-PROCESSES." Journal of Canadian Petroleum Technology **32**(3): 46-52.

Hughes, J. D., et al. (2017). Documentation for the MODFLOW 6 framework: U.S. Geological Survey Techniques and Methods book 6, chap. A57.

Jackson, C. R. (2000). A Novel Grid Refinement Method for Regional Groundwater Flow using Object-Oriented Technology. School of Civil Engineering. Birmingham, University of Birmingham. **PhD**.

Jackson, C. R., et al. (2015). "Evidence for changes in historic and future groundwater levels in the UK." Progress in Physical Geography **39**(1): 49-67.

Jackson, C. R., et al. (2005). "Numerical testing of conceptual models of groundwater flow: a case study using the Dumfries Basin aquifer." Scottish Journal of Geology **41**: 51-60.

Jackson, C. R., et al. (2011). "Modelling the effects of climate change and its uncertainty on UK Chalk groundwater resources from an ensemble of global climate model projections." Journal of Hydrology **399**(1-2): 12-28.

Jackson, C. R. and A. E. F. Spink (2004). User's manual for the groundwater flow model ZOOMQ3D. British Geological Survey Internal Report. **IR/04/140**.

Janssen, S., et al. (2011). "Linking models for assessing agricultural land use change." Computers and Electronics in Agriculture **76**(2): 148-160.

Jones, M. A., et al. (2012). Groundwater resource modelling for public water supply management in London. Groundwater Resources Modelling: A Case Study from the UK. M. G. Shepley, M. I. Whiteman, P. J. Hulme and M. W. Grout, Geological Society London, Special Publications, 364**:** 99-111.

Ju, L. L., et al. (2010). "Voronoi Tessellations and their Application to Climate and Global Modelling, Numerical Techniques for Global Atmospheric Models, Lecture Notes in Computational Science, draft."

Konikow, L. F., et al. (2009). Revised Multi-Node Well (MNW2) Package for MODFLOW Ground-Water Flow Model: U.S. Geological Survey Techniques and Methods, 6-A30, USGS**:** 80.

Langevin, C. D., et al. (2017). Documentation for the MODFLOW 6 Groundwater Flow Model: U.S. Geological Survey Techniques and Methods, book 6, chap. A55.

Le Vine, N., et al. (2016). "Diagnosing hydrological limitations of a land surface model: application of JULES to a deep-groundwater chalk basin." Hydrology and Earth System Sciences **20**(1): 143-159.

Li, J., et al. (2002). Mesh-free method for groundwater modelling. 24th World Conference on Boudnary Element Methods Incorporating Meshless Solutions Seminar, Brebbia, CA, WIT Press Southampton.

Liao, Y. P., et al. (2012). "Integration of urban runoff and storm sewer models using the OpenMI framework." Journal of Hydroinformatics **14**(4): 884-901.

MacDonald, A. M., Brewerton, L.J. and Allen, D.J. (1998). Evidence for rapid groundwater flow and karst-type behaviour in the chalk of south England. Groundwater pollution, aquifer recharge and vulnerability. N. S. Robins, Geological Society Special Publication. **130:** 95-106.

Mansour, M. M., et al. (2011). "Pumping test analysis using a layered cylindrical grid numerical model in a complex, heterogeneoeus chalk aquifer." Journal of Hydrology **401**(1-2): 14-21.

Mathias, S. A., et al. (2008). "Approximate solutions for Forchheimer flow to a well." Journal of Hydraulic Engineering-Asce **134**(9): 1318-1325.

Mathias, S. A. and L. C. Todman (2010). "Step-drawdown tests and the Forchheimer equation." Water Resources Research **46**.

Mathworks (2012). MATLAB Release 2012b. Natick, Massachusetts, USA.

McDonald, M. G. and A. W. Harbaugh (1988). A modular three-dimensional finite-difference groundwater flow model. U.S. Geological Survey Techniques of Water-Resources Investigations. **O6-A1:** 576.

Mehl, S. and M. C. Hill (2002). "Development and evaluation of a local grid refinement method for block-centered finite-difference groundwater models using shared nodes." Advances in Water Resources **25**(5): 497-511.

Mehl, S. and M. C. Hill (2004). "Three-dimensional local grid refinement for block-centered finite-difference groundwater models using iteratively coupled shared nodes: a new method of interpolation and analysis of errors." Advances in Water Resources **27**(9): 899-912.

Mohamed, M. M., et al. (2016). "Groundwater modeling as a precursor tool for water resources sustainability in Khatt area, UAE." Environmental Earth Sciences **75**(5): 18.

Moore, R. V. and C. I. Tindall (2005). "An overview of the open modelling interface and environment (the OpenMI)." Environmental Science & Policy **8**(3): 279-286.

Mortimore, R. N. (1986). "Stratigraphy of the Upper Cretaceous White Chalk of Sussex." Proceedings of the Geologists' Association **97**: 97-139.

Mrosovsky, I., Ridings, R.L (1974). Two-Dimensional Radial Treatment of Wells Within a Three-Dimensional Reservoir Model. SPE-AIME Third Symposium on Numerical Simulation of Reservoir Performance. Houston, Texas, American Institute of Mining, Metallurgical and Petroleum Engineers.

Mundal, S. S., et al. (2010). "Simulation of anisotropic heterogeneous near-well flow using MPFA methods on flexible grids." Computational Geosciences **14**(4): 509-525.

Neale, R. B., et al. (2010). NCAR Technical Note: Description of the NCAR Community Atmosphere Model (CAM 4.0) (NCAR/TN-485+STR).

Palagi, C. L. and K. Aziz (1994). "MODELING VERTICAL AND HORIZONTAL WELLS WITH VORONOI GRID." SPE Reservoir Engineering **9**(1): 15-21.

Palagi, C. L., Aziz, K. (1994). "Use of Voronoi Grid in Reservoir Simulation." SPE Advacned Technology Series **2**(2): 69-77.

Palagi, C. L., Ballin, P.R, Aziz, A. (1993). The Modeling of Flow in Heterogeneous Reservoirs with Voronoi Grid. 12th SPE Symposium on Reservoir Simulation. New Orleans, LA, USA, Society of Petroleum Engineers.

Panday, S., et al. (2013). MODFLOW-USG version 1: An unstructured grid version of MODFLOW for simulating groundwater flow and tightly coupled processes using a control volume finite-difference formulation: U.S. Geological Survey Techniques and Methods, 6-A45, USGS**:** 66.

Panday, S., et al. (2017). MODFLOW-USG version 1.4.00: An unstructured grid version of MODFLOW for simulating groundwater flow and tightly coupled processes using a

control volume finite-difference formulation. USGS Geological Survey Sofware Release, 27 October 2017.

Papadopulos, I. S. and H. H. Cooper (1967). "Drawdown in a well of large diameter." Water Resources Research **3**: 241-244.

Peckham, S. D., et al. (2013). "A component-based approach to integrated modeling in the geosciences: The design of CSDMS." Computers & Geosciences **53**(0): 3-12.

Pedrosa Jr, O. A. and K. Aziz (1986). "Use of a Hybrid Grid in Reservoir Simulation." SPE Reservoir Engineering.

Provost, A. M., et al. (2017). Documentation for the “XT3D” option in the Node Property Flow (NPF) Package of MODFLOW 6: U.S. Geological Survey Techniques and Methods, book 6.

Rathod, K. S. and K. R. Rushton (1991). "Interpretation of pumping from 2-zone layered aquifers using a numerical-model." Ground Water **29**(4): 499-509.

Ringler, T., et al. (2008). "A multiresolution method for climate system modeling: application of spherical centroidal Voronoi tessellations." Ocean Dynamics **58**(5-6): 475-498.

Ringler, T., et al. (2013). "A multi-resolution approach to global ocean modeling." Ocean Modelling **69**: 211-232.

Robinson, N. D. (1986). "Lithostratigraphy of the Chalk Group of the North Downs, southeast England." Proceedings of the Geologists’ Association **97**: 141-170.

Rozon, B. J. (1989). A Generalized Finite Volume Discretization Method for Reservoir Simulation. Reservoir Simulation Symposium. Houston, Texas, Society of Petroleum Engineers.

Rushton, K. R. (2006). "Significance of a seepage face on flows to wells in unconfined aquifers." Quarterly Journal of Engineering Geology and Hydrogeology **39**: 323-331.

Rushton, K. R. and S. J. Booth (1976). "Pumping-test analysis using a discrete time-discrete space numerical-method." Journal of Hydrology **28**(1): 13-27.

Rushton, K. R., et al. (1989). "Estimation of the groundwater resources of the berkshire downs supported by mathematical-modeling." Quarterly Journal of Engineering Geology **22**(4): 329-341.

Rushton, K. R. and K. S. Rathod (1988). "Causes of non-linear step pumping test responses." Quarterly Journal of Engineering Geology and Hydrogeology **21**(2).

Rushton, K. R. and J. Weller (1985). "Response to pumping of a weathered-fractured granite aquifer." Journal of Hydrology **80**(3-4): 299-309.

Safiolea, E., et al. (2011). "Integrated modelling for river basin management planning." Proceedings of the Institution of Civil Engineers-Water Management **164**(8): 405-419.

Salmon, S., et al. (1996). "Development of a groundwater resource model for the Yorkshire Chalk." Journal of the Chartered Institution of Water and Environmental Management **10**(6): 413-422.

Shampine, L. F. and M. W. Reichlet (1997). "The MATLAB ODE Suite." SIAM Jounral of Scientific Computing **18**(1): 1-22.

Shepley, M., et al. (2012). Groundwater Resources Modelling: A Case Study from the UK. London, GSL.

Sherif, M., et al. (2012). "Modeling Groundwater Flow and Seawater Intrusion in the Coastal Aquifer of Wadi Ham, UAE." Water Resources Management **26**(3): 751-774.

Shrestha, N. K., et al. (2014). "Modelling Escherichia coli dynamics in the river Zenne (Belgium) using an OpenMI based integrated model." Journal of Hydroinformatics **16**(2): 354-374.

Shrestha, N. K., et al. (2013). "OpenMI-based integrated sediment transport modelling of the river Zenne, Belgium." Environmental Modelling & Software **47**: 193-206.

Singh, A. (2014). "Groundwater resources management through the applications of simulation modeling: A review." Science of the Total Environment **499**: 414-423.

Szekely, F. (1998). "Windowed spatial zooming in finite-difference ground water flow models." Ground Water **36**(5): 718-721.

Tamayo-Mas, E., et al. (2018). "Impact of model complexity and multi-scale data integration on the estimation of hydrogeological parameters in a dual-porosity aquifer." Hydrogeology Journal.

Thiem, G. (1906). Hydrologische Methoden. Gebhardt, Leipzig.

Upton, K. A., et al. (2019). "Modelling boreholes in complex heterogeneous aquifers." Environmental Modelling & Software.

von Rosenberg, D. U. (1982). Local Mesh Refinement for Finite Difference Methods SPE 10974. 57th Annual Fall Technical Conference and Exhibition of the Society of Petroleum Engineers. New Orleans, Society of Petroleum Engineers of AIME.

Wang, H. F. and M. P. Anderson (1982). Introduction to Groundwater Modelling: Finite Difference and Finite Element Methods. London, Academic Press Ltd.

Wen, Z., et al. (2014). "Numerical modeling of Forchheimer flow to a pumping well in a confined aquifer using the strong-form mesh-free method." Hydrogeology Journal **22**(5): 1207-1215.

Williams, A., et al. (2006). "Characterising the vertical variations in hydraulic conductivity within the Chalk aquifer." Journal of Hydrology **330**(1-2): 53-62.

WWAP (2015). The United Nations World Water Development Report 2015: Water for a Sustainable World. Paris, UNESCO.

Zhou, Z., et al. (2013). "An OpenMI-based combined model for alongshore sediment transport and shoreline change." Proceedings of the Institution of Civil Engineers-Maritime Engineering **166**(4): 175-186.

Zhu, Z. D., et al. (2016). "Integrated urban hydrologic and hydraulic modelling in Chicago, Illinois." Environmental Modelling & Software **77**: 63-70.